Counting Red Blood Cells in Thin Blood Films: A Comparative Study

Alan Klinger Sousa Alves[1][a] and Bruno Motta de Carvalho[2][b]

[1] *Instituto Federal de Educação, Ciência e Tecnologia do Rio Grande do Norte - Campus Nova Cruz, Av. José Rodrigues de Aquino Filho, Nova Cruz, Brazil*

[2] *Departamento de Informática e Matemática Aplicada, Universidade Federal do Rio Grande do Norte, Rua Cel. João Medeiros, Natal, Brazil*

Keywords: Malaria, Computer Vision, RBC Counting.

Abstract: Malaria is a disease caused by a parasite that is transmitted to humans through the bites of infected mosquitoes. There were an estimated 247 million cases of malaria in 2021, with an estimated number of 619,000 deaths. One of the tasks in diagnosing malaria and prescribing the correct course of treatment is the computation of parasitemia, that indicates the level of infection. The parasitemia can be computed by counting the number of infected Red Blood Cells (RBCs) per μL or the percentage of infected RBCs in 500 to 2,000 RBCs, depending on the used protocol. This work aims to test several techniques for segmenting and counting red blood cells on thin blood films. Popular methods such as Otsu, Watershed, Hough Transform, combinations of Otsu with Hough Transform and convolutional neural networks such as U-Net, Mask R-CNN and YOLO v8 were used. The results obtained were compared with two other published works, the Malaria App and Cell Pose. As a result, one of our implemented methods obtained a higher F1 score than previous works, especially in the scenario where there are clumps or overlapping cells. The methods with the best results were YOLO v8 and Mask R-CNN.

1 INTRODUCTION

Malaria is a disease caused by a parasite of the genus *Plasmodium* and it is transmitted by some mosquitoes of the genus Anopheles (Giacometti et al., 2021). The main method for diagnosing malaria infections is optical microscopy (Organization et al., 2021). In order to have the right course of treatment, it is necessary to determine the specie of the plasmodium, the stage of the disease and parasitemia of the sample. Thus, it is important to make a proper estimate, as both an overestimation or an underestimation can be equally harmful (Eziefula et al., 2012). The parasitemia is computed as a percentage of infected Red Blood Cells (RBCs) relative to the total number of red blood cells (Organization et al., 2021). Thus, a high accuracy in the red blood cell counting process is very important for achieving accurate parasitemia results.

Estimating parasitemia from thin blood films has been addressed in several studies (Rehman et al., 2018). However, there is still room for improvement, specially in the case of clumped or overlapped cells

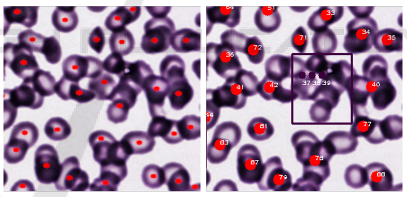
a) Cell Pose b) Malaria App

Figure 1: Both tools present difficulty in individually identifying each RBC in the scenario with overlapped cells.

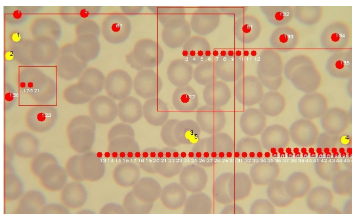
Figure 2: The Malaria App makes a rectangle around the cells and then estimates the number of cells in the area. This estimate may not be very efficient.

(Rehman et al., 2018). Figure 1 shows the result of the RBC segmentation of two published methods for the same sample, on the left side, Figure 1a, we have the segmentation generated by Cell Pose (Stringer

[a] https://orcid.org/0000-0003-2501-4751
[b] https://orcid.org/0000-0002-9122-0257

Alves, A. and Motta de Carvalho, B.
Counting Red Blood Cells in Thin Blood Films: A Comparative Study.
DOI: 10.5220/0012455000003657
Paper published under CC license (CC BY-NC-ND 4.0)
In *Proceedings of the 17th International Joint Conference on Biomedical Engineering Systems and Technologies (BIOSTEC 2024) - Volume 2*, pages 687-694
ISBN: 978-989-758-688-0; ISSN: 2184-4305
Proceedings Copyright © 2024 by SCITEPRESS – Science and Technology Publications, Lda.

et al., 2021) and on the right side, Figure 1b, we have the segmentation from Malaria App (Oliveira, 2019), Both present poor results in the scenario where the cells are very close to each other, with the red dots indicating which cells were identified. In this case many cells went unnoticed. This problem is reported in several other works (Rehman et al., 2018).

In the case of the Malaria App (Oliveira, 2019), there is still a worst case scenario that can be seen in the Figure 2, that happens when the algorithm cannot break down clumps of red blood cells and produces an estimative of the number of cells in an area marked by a rectangle. In this case, it is possible that the method produces a lower quality estimate, with a larger error, that can affect the computed parasitemia.

The objective of this work is to propose alternate methods for counting RBCs in thin blood films and analyze their results, in order to obtain more accurate parasitemia estimates. Section 2 presents some related works while Section 3 briefly describes the implemented methods. Section 4 presents the results and a discussion about them. Finally, Section 5 presents our conclusion and suggests future work for this task.

2 RELATED WORK

One of the main related works is the Malaria App (Oliveira et al., 2018) (Oliveira, 2019), which employed an adaptive version of the Otsu threshold (Otsu, 1979) to produce binary images, segmenting the RBCs from the background. Morphology operations such as hole filling, dilation and erosion were performed to fill up cells and break down connected cells, these operations are already known and recommended (Wu et al., 2010). Finally, clumps of cells are identified and the number of RBCs in each clump are estimated based on the area and border length of the clump. The infected cells and white cells are detected using a Hue, Saturation and value (HSV) filter, since the malaria samples are stained with the Giemsa dye.

Another important related work is Cell Pose (Stringer et al., 2021) which used a generalist approach through a convolutional neural network based on an U-Net. Approximately 510 images of microscopic objects were used for training, but not all of them are of blood cells. Cell Pose was tested and compared to other state-of-the-art tools, obtaining results superior to all. The comparisons were performed against the results produced by Stardist (Schmidt et al., 2018), Mask R-CNN (He et al., 2017) (Abdulla, 2017) and the U-Net (Ronneberger et al., 2015) with two and three classes. A test was carried out with 111 images similar to our study, and Cell Pose achieved an accuracy of 93% in the Intersection Over Union (IoU) metric, while Mask R-CNN achieved 82% and Stardist achieved 75%.

In another study, (Devi et al., 2018) proposed a method for detecting infected erythrocytes that uses Otsu's thresholding to obtain binary images of the thin blood samples, followed by a Watershed segmentation. Then, they extracted 54 features that are fed to several feature selection techniques to remove irrelevant data. The selected features are used to train several different classifiers (SVM, *k*-NN and Naive Bayes) that are also combined in hybrid classifiers. It is important to note that that method only detects the infected cells and does not count all the RBCs.

The RBC and white blood cells (WBC) counts are also important for the diagnosis of other diseases such as leukemia, allergies, tissue injuries, bronchogenic infection, anemia and even kidney tumors and lung diseases (Society, 2023). For this reason, there are several studies that seek to count RBC or WBC. The techniques for both are similar, where some of the techniques being used are based on separation by colors on the Hue, Saturation and Intensity (HSI) color space or the L*a*b* color space, or on machine learning techniques such as K-Means, Fuzzy C-Means or convolutional neural networks (CNNs) (Tran et al., 2018).

A combination of Ycbcr space Color conversion was used in conjunction with a circle Hough Transform and watershed algorithm, with this method obtaining an accuracy of 90.98% in Acute lymphoblastic leukemia image database (ALL-IDB) (Yeldhos et al., 2018). Using the same data set, another work applied a SegNet obtaining an accuracy rate of 85.50% for WBC and 82.9% for RBC (Tran et al., 2018).

The network You Only Look Once (YOLO) version 2 was also used for WBC detection, achieving a detection accuracy of 96% (Abas et al., 2021), to 100% (Wang et al., 2018). It is important to note that the WBC detection problem is simpler than RBC segmentation, as some samples have many objects overlapping each other in the latter case.

In this work, we also use convolutional networks such as the U-Net (Ronneberger et al., 2015) which has the advantage of producing better results when working with fewer samples when compared to other convolutional neural networks (CNNs), the Mask R-CNN (Abdulla, 2017), which is an extension of a R-CNN that adds the object mask prediction and the newest version of the YOLO, the YOLO v8 (Jocher et al., 2023).

3 METHODOLOGY

This work began by obtaining the same data set used in the Malaria App project (Oliveira, 2019), then we started with the implementation of traditional methods that did not use neural networks using only Python and OpenCV. The data set consists of 30 samples that were stained with the Giemsa dye and imaged using a standard optical microscope using a 1000× zoom, the standard protocol for diagnosing malaria. The images were originally captured with a resolution of 2592 × 1944, and reduced to 640 × 480 in our case, since the detection and counting of RBCs do not need a high resolution image.

Now, we proceed by briefly describing the used algorithms.

3.1 Otsu

Otsu's method (Otsu, 1979) is an algorithm for determining an optimal threshold for separating pixels from an image into two classes. It has been extensively used in its original form and in adaptive ways, usually by subdividing the image into blocks, thus, avoiding problems caused by non-uniform illumination and contrast.

It was noticed that in this method the blurring filter was bringing together the edges of some cells. It is possible to see an example of this effect in Figure 3, we have a group indicated by the yellow arrow with the wrong estimate, they should have 4 cells but 3 were estimated. In Figure 4, fewer cells were included in the group, thus, the estimate obtained the correct answer, in this Figure we have the same method, but without the blur. In general, even without blurring the image, this method generates many groups of cells, which cannot be segmented individually, having to resort to making an estimate, similar to what was implemented in Malaria App. This estimate can be quite wrong when the group contains many cells.

In both Figures it is also possible to notice another problem: this method captures practically any object, for example, the spot in the center of both Figures 3 and 4 that was identified as a group of cells, therefore, this will generate many false positives. In this work we generate results for Otsu Adaptive, which in the tables appears labeled as Otsu and for Otsu Adaptative with Gaussian blur, which in the tables appears labeled as Otsu + Gaussian blur.

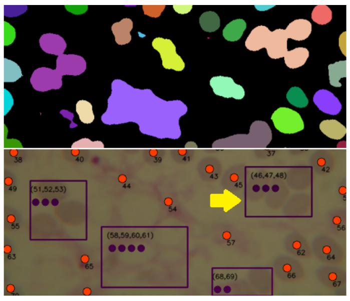
Figure 3: Segmentation with Otsu + Gaussian blur, the spots are identified as cells and the estimation of the group identified by the yellow arrow is flawed.

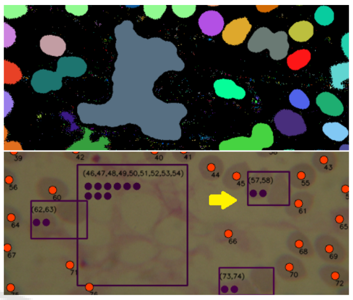
Figure 4: Segmentation with Otsu, the groups of cells identified by the yellow arrow became smaller and the estimation improved.

3.2 Watershed

The Watershed algorithm views an image as a topographic surface in which high intensities denote peaks and hills while low intensities denote valleys, and gradually fills the valleys until the water from different regions merge. Then, an "artificial dam" is built between them and determine boundaries between objects.

Figure 5 shows the result of the Watershed algorithm, that generates something similar to a relief map of the image (left) and the RBC labeling on the right. Note that although some cells appear to be together, it manages to separate them. One of the problems noticed is that it has difficulty finding cells that are very clear and in some cases it generates groups of cells.

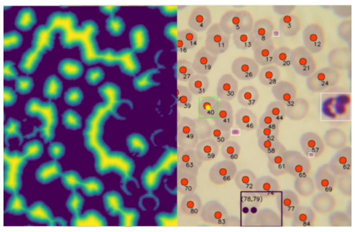
Figure 5: Watershed segmentation can individually identify some cells that are very close to each other, but has difficulty identifying very light cells.

Watershed also doesn't make a good distinction between sample objects. In Figure 6 with sample C, we can see 8 false positives.

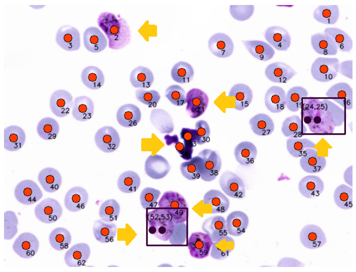

Figure 6: Yellow arrows show incorrect classifications with Watershed, any object is incorrectly classified as a cell.

3.3 Circle Hough Transform

This method uses the circle Hough Transform from Python's OpenCV library to identify circles in the sample. The difficulty of the method is the configuration of the parameters. Figure 7 shows the result of the method with each circle that was found in sample B, the perceived problem is that this method finds circles in places where there are no cells, generating false positives. We indicate this problem with yellow arrows. Furthermore, this method has difficulty capturing cells that are not in an approximate circular shape.

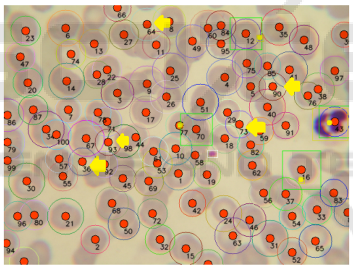

Figure 7: Empty spaces can be classified as cells if objects in the surrounding environment form something like a circle, the yellow arrows point out these problems.

In Figure 8 we have a sample with 7 false positives, in which we can observe that the circle Hough Transform will capture any object that is in a circular format, making no distinction between contaminated cells, WBCs and RBCs.

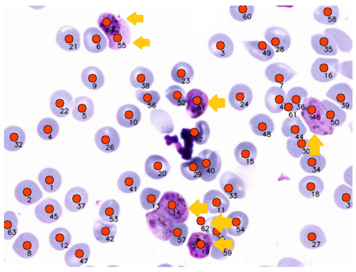

Figure 8: Incorrect classification with circle Hough Transform, any circular shaped object is identified as a cell, as highlighted by the yellow arrows.

3.4 Otsu + Circle Hough Transform

We noted that the circle Hough Transform and Otsu could overcome some of each other's deficiencies, since the circle Hough Transform can identify cells individually, even if they are very close, while Otsu can identify cells that are in different formats, so we decided to test two methods that would unite Otsu and the circle Hough Transform.

The first method would be, after using Otsu, instead of trying to make an estimate to identify the number of cells in the groups that could not be separated, use circle Hough Transform to break down the groups of cells generated. In this way we implemented Otsu + Hough 1, whose result for a sample can be seen in Figure 9. The Figure 9a shows that Otsu created several groups, while in Figure 9b there is the same sample with the result generated by Otsu + Hough 1. there, it is possible to see that all groups were individually segmented with only 8 false positives indicated by the yellow arrows.

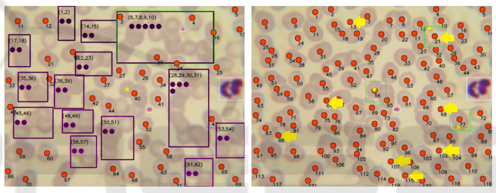

a) Otsu b) Otsu + Hough 1

Figure 9: Segmentation with Otsu + Hough 1, figure (a) shows the result of Otsu, figure (b) shows the result of Otsu after breaking the cell groups with the circle Hough Transform. Yellow arrows highlight false positives.

The second method would simply be to combine the Otsu result with circle Hough Transform, we call this method Otsu + Hough 2, this second method generates fewer false positives, but finds fewer cells than the previous method. A result of its use can be seen in Figure 10.

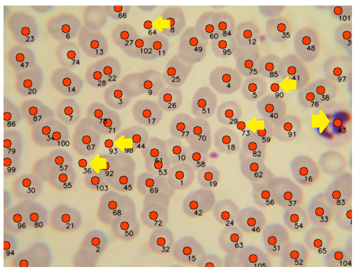

Figure 10: Segmentation with Otsu + Hough 2, this combination is the simple sum of the results of the two methods, consequently there will be errors present in both methods. Yellow arrows highlight false positives.

3.5 Mask R-CNN

Mask R-CNN (Abdulla, 2017) was the slowest method, with its execution taking about 1 minute and 30 seconds to segment just one sample. This time does not preclude its use, but it is important to highlight it. This network obtained good results, with two examples being shown on Figure 11. It is possible to see that it generates few false positives and does not generate groups of cells.

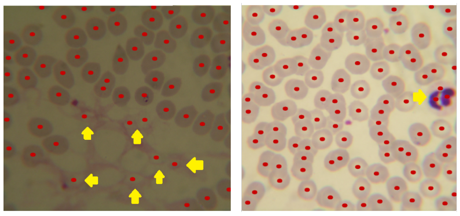
a) Sample A b) Sample B

Figure 11: Mask R-CNN was not able to accurately differentiate cells from spots and others objects. Yellow arrows highlight problems.

Despite the good results with images with clumps of cells, Mask R-CNN also presented a problem: it considers most objects as RBCs. In sample C presented in Figure 12, it is possible to observe at least 11 objects that were erroneously classified as RBCs. The problem occurs in most samples and can also be seen in Figure 11.

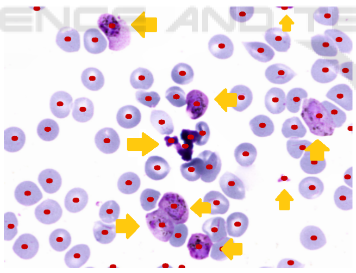
Figure 12: Wrong classification with Mask R-CNN, this neural network is also not capable of differentiating cells from other objects in the samples. Yellow arrows highlight problems.

3.6 U-Net

U-Net is also a convolutional network, with a big advantage that it is fast to train and requires fewer images to obtain a good result when compared to other CNNs. Figure 13 exemplifies its use with two samples. It was one of the only methods that did not generate false positives, managing to precisely differentiate the cells from spots. In Figure 13b, does not generate false positives, however, it finds fewer cells than actually exist in the image.

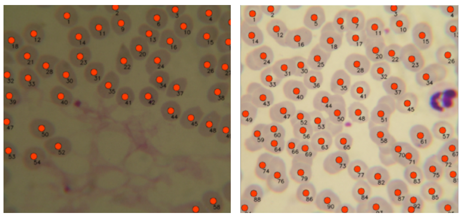
a) Sample A b) Sample B

Figure 13: For these samples, U-Net can differentiate spots and others objects from cells.

Like Mask R-CNN, U-Net also captures many objects such as RBCs, but in smaller quantities, Figure 14 is the same sample as Figure 12 but with only 6 false positives. Just by looking at Figure 13 it would not be possible to observe this problem.

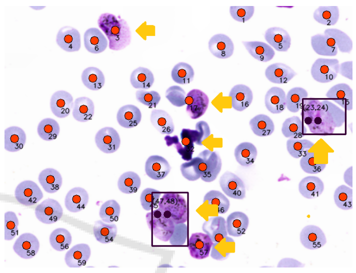
Figure 14: U-Net cannot differentiate cells from other objects when they are very similar to them. False positives are indicated with yellow arrows.

3.7 YOLO v8

The version 8 of YOLO at the moment is the latest one of this convolutional network. This network had a reasonable training time, but the segmentation execution takes less than 1 second. Figure 15 shows that it generated some false positives in sample A, but it was the only method that found all RBCs in the sample B.

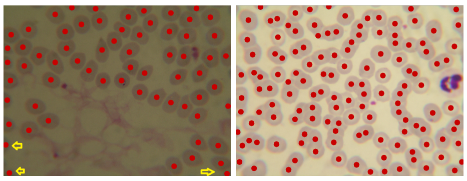
a) Sample A b) Sample B

Figure 15: The segmentation with YOLO v8 made only a few false positives in the image (a) highlighted by the yellow arrows and managed to find all the red blood cells in the image (b).

Unlike the two previous convolutional networks, YOLO v8 correctly classifies most objects, an example can be seen in Figure 16, where there are no false positives.

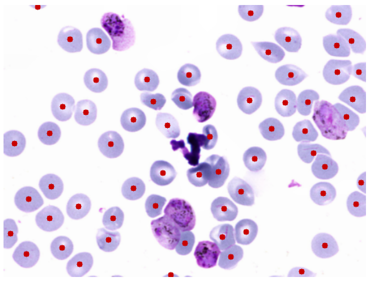

Figure 16: Good classification with YOLO v8. It was possible to differentiate even cell-like objects.

4 EXPERIMENTS

In this session we describe the experiments performed, the metrics used for comparing the results and present the results.

After testing traditional algorithms for segmentation, we started testing with convolutional networks such as U-Net, Mask R-CNN and YOLO v8. In order to train a more general model, an additional 400 microscopic images were obtained, of which 100 would be used only for validation and comparison of the methods. With these 330 images, data augmentation was carried out with rotations and mirroring, generating 2,860 images. The experiments were performed on a computer equipped with 40 Intel Xeon E5-2660 CPUs and with 64GB of RAM.

Resolutions of 256, 384, 416, 512 and 1024 were tested for the convolutional networks, however data will only be presented for the resolutions that provided the best results.

The U-Net took 28 hours to train for 1,500 epochs using Tensorflow (Abadi et al., 2015), Adam optimizer (Kingma and Ba, 2014) and binary cross entropy as the loss function with the resolution of 256×256. A total of 2,145 images were used for training and 715 for validation.

For the Mask R-CNN training, we used the same parameters used in U-Net, 2,145 images for training and 715 for validation, the best resolution was 1024×1024. The initial weights were the same as the ones used on ImageNet, and we used 20 epochs for the net head and 40 epochs for the other layers. Each epoch had 100 steps of training, using the ResNet50's backbone. The whole training took approximately 6 days.

For the YOLO v8, we used 1,425 images for training, 804 for validation and 631 for testing. The training used 2,000 epochs with a batch size of 25 and the best resolution was 512×512, in about 59 hours.

4.1 Comparing Results

Our objective was not to perform an exact segmentation, but rather a precise count of the RBCs in the sample, for this reason, we did not use the Intersection over Union (IoU) metric.

We created a tool to compare the evaluated image and the ground truth, based on the position of each RBC. All segmentation algorithms mark each RBC with a red circle, the comparison tool searches for these circles, comparing the position of each one with the closest RBC to the same position in the ground truth. When an RBC is found in the same position in both the ground truth and the evaluated image, a green circle is made above and a number is added, so that it is possible to check exactly whether the RBC in that position corresponds to the RBC in the same position in the other image. This comparison can be seen in Figure 17, where on the left side (a) we have the image being evaluated and on the right side (b) we have the ground truth.

Some algorithms, such as the Malaria App or Watershed, generate groups of cells and make an estimate for each group. In these cases, a yellow square is added with the count of the group's RBCs in the evaluated image, the example can be seen in Figure 17(a), where we have 1 purple rectangle with the count highlighted in a yellow square and in the ground truth image the RBCs within the group area are painted light green, which can also be seen in Figure 17(b).

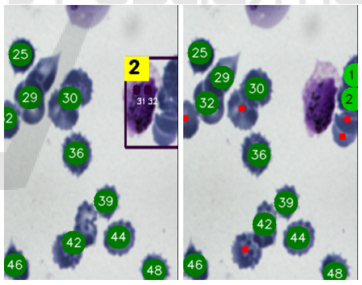

a) Malaria App b) Ground truth

Figure 17: (a) Results from (Oliveira, 2019) . (b) Ground truth image, dark green circles mark cells that were correctly identified, the light green circles in identify the cells that were "extracted" from RBC groups, while the smaller red circles identify the cells that were not detected.

Therefore, the red circles that remain in the image being evaluated are considered false positives and those that remain in the ground truth image are false negatives. Additionally, a 50px border was created around the image to avoid considering RBCs that are very close to the edge, because the count made by an expert would not evaluate these RBCs as they are only partially seen.

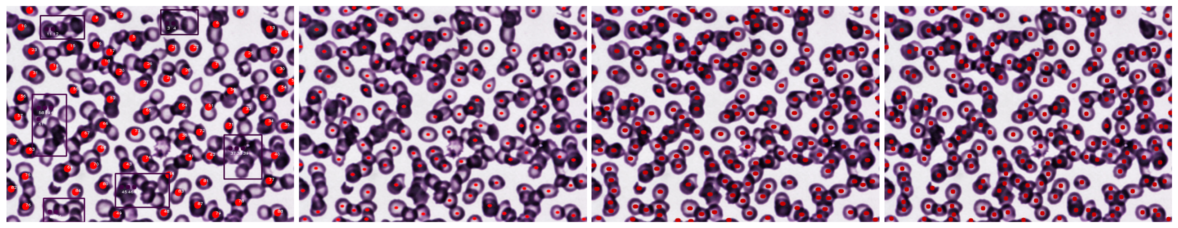

Figure 18: Segmentation of a complex sample with 199 RBCs: Malaria App found 84 RBCs, Cell Pose found 113 RBCs, Mask R-CNN found 172 RBCs and YOLO v8 found 183 RBCs.

4.2 Results

As most methods only took average execution times between 0.5 and 1.5 seconds per sample, we consider the time differences as negligible and do not report on them. Table 1 presents the precision, recall and F1 scores accuracies for all methods tested.

Table 1: Precision, recall and F1 scores.

Method name	Precision	Recall	F1
Hough Transform	0.928	0.817	0.861
Otsu + Gaussian blur	0.898	0.763	0.817
OTSU + Hough 1	0.869	0.887	0.872
OTSU + Hough 2	0.907	0.874	0.886
OTSU	0.902	0.771	0.824
Mask R-CNN	0.919	**0.980**	0.948
U-Net	0.916	0.842	0.873
Watershed	0.895	0.904	0.894
YOLO v8	**0.942**	0.976	**0.958**
Malaria App	0.897	0.842	0.862
Cell Pose	0.936	0.943	0.936

Among the methods tested by us, YOLO v8 obtained the best result in precision and F1 score (0.942) and (0.958) respectively, followed by circle Hough Transform with the second highest precision (0.928) and Mask R-CNN with the second best F1 score (0.948). Regarding Recall, Mask R-CNN obtained the best result (0.980), followed by YOLO v8 (0.976).

However, we have to emphasize that the parasitemia computation is an easier task than the classification task which we are reporting. In the counting task, a false positive and a false negative in the same sample cancel each other, while in the classification task, they count as two errors. Therefore, we present Table 2 that shows the average percentage of errors for each implemented method. The errors are counted in a simpler way: if in the sample there are 10 cells and the algorithm identified 12 or 8 the error will be 2. To calculate this percentage, the difference between the expected count for each sample and the count carried out by each method was computed, and only then the percentage of this difference was calculated. According to Table 2, of the methods tested by us, YOLO v8 managed to have the best error average with just 5.02% followed by Mask R-CNN (8.28%), while Malaria App had an average error rate of 11.22% and Cell Pose had an error rate of 6.81%.

Table 2: Methods error percentage average.

Method	Percent error
Circle Hough Transform	15.539
Otsu + Gaussian blur	18.066
Otsu + Hough 1	13.659
Otsu + Hough 2	10.754
Otsu	18.375
Mask R-CNN	8.281
U-Net	11.461
Watershed	10.596
YOLO v8	**5.025**
Malaria App	11.220
Cell Pose	6.812

In simple samples, most methods present a good result, and the big difference occurs in samples with clumped or overlapped cells. Figure 18 presents the result of segmentation by the two published methods and the two best methods implemented by us, in one of the more challenging samples. This sample has 199 RBCs, while Malaria App found only 84 and Cell Pose found 113, our Mask R-CNN and YOLO v8 found 172 and 183 respectively.

Cell Pose presents an smaller percent error value than Mask R-CNN because most of the samples used in this study are simple. If the majority were more complex, the Mask R-CNN's percent error would probably be smaller than Cell Poses's percent error.

5 CONCLUSIONS

The results show the YOLO v8 and Mask R-CNN as the most accurate ones. The big difference between these two methods compared to Malaria App and Cell Pose is in dealing with clumped and overlapped RBCs, in which cases both tools present lower accuracies than YOLO v8 and Mask R-CNN.

As future work, we intend to train convolution networks to deal specifically with the problem of clumped groups of RBCs, the main problem in this task. Moreover, we believe that the problem may be simplified with a better designed pre-processing phase, with more robust hole filling and cell separation procedures. This approach will also be further investigated.

To have an even more generic CNN, we could add more images to the training dataset. The difficulty lies in obtaining and labeling each image, as it is a time-consuming process. Furthermore, other datasets will need to be created to identify other diseases, so the labeling process needs to be improved. So, as we already have a CNN capable of identifying RBCs, we can use the prediction result as a starting point to label more samples in a semi-automatic approach, drastically reducing the labeling time.

REFERENCES

Abadi, M., Agarwal, A., Barham, P., et al. (2015). TensorFlow: Large-scale machine learning on heterogeneous systems. Software available from tensorflow.org.

Abas, S. M., Abdulazeez, A. M., and Zeebaree, D. (2021). A yolo and convolutional neural network for the detection and classification of leukocytes in leukemia. *Indones. J. Electr. Eng. Comput. Sci*, 25(1).

Abdulla, W. (2017). Mask R-CNN for object detection and instance segmentation on keras and tensorflow. https://github.com/matterport/Mask_RCNN.

Devi, S. S., Roy, A., Singha, J., Sheikh, S. A., and Laskar, R. H. (2018). Malaria infected erythrocyte classification based on a hybrid classifier using microscopic images of thin blood smear. *Multimed. Tools Appl.*, 77(1):631–660.

Eziefula, A. C., Gosling, R., Hwang, J., Hsiang, M. S., Bousema, T., Von Seidlein, L., and Drakeley, C. (2012). Rationale for short course primaquine in africa to interrupt malaria transmission. *Malaria J.*, 11:1–15.

Giacometti, M., Milesi, F., Coppadoro, P. L., Rizzo, A., Fagiani, F., Rinaldi, C., Cantoni, M., Petti, D., Albisetti, E., Sampietro, M., et al. (2021). A lab-on-chip tool for rapid, quantitative, and stage-selective diagnosis of malaria. *Adv. Sci.*, page 2004101.

He, K., Gkioxari, G., Dollár, P., and Girshick, R. (2017). Mask R-CNN. In *Proceedings of the ICCV*, pages 2961–2969.

Jocher, G., Chaurasia, A., and Qiu, J. (2023). YOLO by Ultralytics.

Kingma, D. P. and Ba, J. (2014). Adam: A method for stochastic optimization. *ArXiv preprint arXiv:1412.6980.*

Oliveira, A. D., Carvalho, B. M., Prats, C., Espasa, M., i Prat, J. G., Codina, D. L., and Albuquerque, J. (2018). An automatic system for computing malaria parasite density in thin blood films. In *Progress in Pattern Recognition, Image Analysis, Computer Vision, and Applications*, pages 186–193. Springer International Publishing.

Oliveira, A. D. d. (2019). *MalariaApp: Um sistema de baixo custo para diagnóstico de malária em lâminas de esfregaço sanguíneo usando dispositivos móveis*. PhD thesis, Universidade Federal do Rio Grande do Norte.

Organization, W. H. et al. (2021). Who guideline for malaria, 13 july 2021. Technical report, World Health Organization.

Otsu, N. (1979). A threshold selection method from gray-level histograms. *IEEE Trans. on Syst. Man Cybern.*, 9(1):62–66.

Rehman, A., Abbas, N., Saba, T., Mehmood, Z., Mahmood, T., and Ahmed, K. T. (2018). Microscopic malaria parasitemia diagnosis and grading on benchmark datasets. *Mic. Res. Tech.*, 81(9):1042–1058.

Ronneberger, O., Fischer, P., and Brox, T. (2015). U-Net: Convolutional networks for biomedical image segmentation. In *Pro. of MICCAI*, pages 234–241. Springer.

Schmidt, U., Weigert, M., Broaddus, C., and Myers, G. (2018). Cell detection with star-convex polygons. In *Proc. of MICCAI*, pages 265–273. Springer.

Society, C. C. (2023). Complete blood count (CBC). https://cancer.ca/en/treatments/tests-and-procedures/complete-blood-count-cbc#ixzz5JmJ8jOk9. Accessed: 2023-08-28.

Stringer, C., Wang, T., Michaelos, M., and Pachitariu, M. (2021). Cellpose: A generalist algorithm for cellular segmentation. *Nat. Methods*, 18(1):100–106.

Tran, T., Kwon, O.-H., Kwon, K.-R., Lee, S.-H., and Kang, K.-W. (2018). Blood cell images segmentation using deep learning semantic segmentation. In *Proc. of the ICECE*, pages 13–16. IEEE.

Wang, X., Xu, T., Zhang, J., Chen, S., and Zhang, Y. (2018). So-yolo based wbc detection with fourier ptychographic microscopy. *IEEE Access*, 6:51566–51576.

Wu, Q., Merchant, F., and Castleman, K. (2010). *Microscope Image Processing*. Elsevier.

Yeldhos, M. et al. (2018). Red blood cell counter using embedded image processing techniques. *Res. Rep.*, 2.